Analytical structure of the S matrix for the coupled channel problem $d + t \leftrightarrow n + \alpha$ and the interpretation of the $J^\pi = \frac{3}{2}^+$ resonance in ^{5}He

L. N. Bogdanova
Institute of Theoretical and Experimental Physics, Moscow, 117259, U.S.S.R.

G. M. Hale
Theoretical Division, Los Alamos National Laboratory, Los Alamos, New Mexico 87545

V. E. Markushin
Kurchatov Atomic Energy Institute, Moscow, 123182, U.S.S.R.

(Received 12 June 1991)

Using a resonance coupled channel model that provides a good description of the experimental data on the reaction $d + t \leftrightarrow n + \alpha$ and d-t elastic scattering in the region of the resonance $^5\mathrm{He}(\frac{3}{2}^+)$, we find the disposition of the S-matrix poles on the different Riemann sheets. An investigation of the motion of the poles with variation of the coupling strengths reveals the structure of the resonant state. The role of scattering and confined channels in the formation of the physical resonance is considered with the use of the probability sum rule for the confined channel. We demonstrate that the resonance $^5\mathrm{He}(\frac{3}{2}^+)$ proves to be a coupled channel pole associated predominantly with the d-t system.

I. INTRODUCTION

The $^3\mathrm{H}(d,n)^4\mathrm{He}$ reaction has been studied extensively at low energies near the $J^\pi = \frac{3}{2}^+$ resonance. Typically the resonance has been parametrized in terms of the usual Breit-Wigner amplitude,

$$S_{12} = \frac{i[\Gamma_1\Gamma_2]^{1/2}}{E_r - E - i\Gamma/2}, \tag{1}$$

with partial widths $\Gamma_1 = \Gamma_2 = 50$ keV in the d-t and n-α channels, respectively, total width $\Gamma = 100$ keV, and resonance energy $E_r = 60$ keV [1] (all energies are given in the center-of-mass system relative to the d-t threshold). This parametrization would imply a resonance pole in the same position, $E_0 = E_r - i\Gamma/2$, on all the sheets (including the physical sheet) of the Riemann energy surface. However, it is known from the general considerations [2–5] of the S matrix that resonances can occur only on the unphysical sheets of the Riemann energy surface, and that they can in principle have different positions on different sheets.

The first indication that the simple Breit-Wigner description of the $\frac{3}{2}^+$ resonance was inadequate came from an R-matrix analysis [6] of the ^{5}He system that included cross-section and polarization data for all three independent reactions involving d-t and n-α at excitation energies below 21.5 MeV. The S-matrix poles corresponding to the $\frac{3}{2}^+$ resonance in ^{5}He from that analysis were found [7] to occur on only two of the unphysical sheets in rather different positions. The main pole, located at $E_R = (47.0 - i37.1)$ keV on the unphysical sheet closest to the physical one ($U_{(1,2)}$ in the notation of Ref. [2]), had the properties of a "conventional" resonance, with partial widths that summed approximately to the total width. The shadow pole, located at $E_S = (81.6 - i3.6)$ keV on the somewhat remote sheet $U_{(2)}$, had much stranger properties. Although very close to the real axis, it produced no narrow structure in the cross section, but was in fact responsible, through its associated zero on the physical sheet, for driving the cross section for the $^3\mathrm{H}(d,n)^4\mathrm{He}$ reaction close to its unitary maximum at the peak of the resonance.

In Ref. [7] it was concluded, using the arguments of Eden and Taylor [2], that the location of the shadow pole implied that in the absence of the coupling between d-t and n-α channels, the $\frac{3}{2}^+$ resonance would be entirely in the n-α channel. Later calculations by Pearce and Gibson [8] indicated that this argument is valid only when the coupling between channels is sufficiently weak that none of the poles changes sheets as coupling strength increases. They speculated that this might not be the case for the coupled d-t and n-α channels, although they did not attempt to find parameters that approximated the physical behavior of the system near the resonance. More recently, Karnakov *et al.* [9] used an effective range expansion to analyze cross sections for the $^3\mathrm{H}(d,n)^4\mathrm{He}$ reaction and for d+t elastic scattering over the resonance. They found, in contradiction to the result of Ref. [7], that the shadow pole occurs on the sheet $U_{(1)}$, rather than on $U_{(2)}$.

In this paper we wish to use the resonance coupled channel model (RCCM) [10], similar in some respects to the separable-potential model of Pearce and Gibson [8], to study specifically the coupled channel system $(d + t, n + \alpha)$ near the resonance. Unlike the usual cou-

pled channel potential model, however, the RCCM introduces explicitly the resonance character of the reaction, allowing its effects to be separated from those of channel coupling and of the Coulomb singularities. The physical values of the model parameters have been determined by comparing with the R-matrix amplitudes for $J^\pi = \frac{3}{2}^+$. The S-matrix pole structure found at physical parameter values confirms that of the previous R-matrix work. More importantly, by varying the strength of the potentials coupling the channels with the ^{5}He resonance away from their physical values, we have generated the trajectories of all the S-matrix poles on the complex energy surface. These trajectories provide a definite answer to the question about the position of the poles in the absence of channel coupling, and also give strong insight into the dynamical origin of the d-t resonance itself. It is found, confirming the conjecture of Pearce and Gibson [8], that the shadow pole indeed changes sheets as the channel coupling strengths are increased to their physical values, and that the $J^\pi = \frac{3}{2}^+$ resonance of ^{5}He arises from the singularities associated with the coupling potential, rather than those associated with the "bare" ^{5}He* state or with the Coulomb interaction in the d-t channel. A description of the model and the way the physical values of its parameters were determined are given in Sec. II. Section III reviews the prescriptions for obtaining S-matrix poles from the model. Section IV contains the main results of the calculation, describing what happens as the coupling strength is varied from zero to the strong-coupling regime. The probability sum rule is considered in Sec. V. Finally, the summary and conclusions of the calculations are given in Sec. VI.

II. THE RESONANCE COUPLED CHANNEL MODEL

A. Model description

We consider the three-channel problem where channel 1 corresponds to the quartet ($s = \frac{3}{2}$) S-wave state of the d-t system, channel 2 corresponds to the doublet ($s = \frac{1}{2}$) D-wave state of the n-α system, and channel 3 consists of a single confined state, the bare resonance ^{5}He*, having total angular momentum and parity $J^\pi = \frac{3}{2}^+$. We define the Hamiltonian to be of the form [10]

$$\mathcal{H} = \begin{pmatrix} H_1 & 0 & V_1 \\ 0 & H_2 & V_2 \\ V_1^\dagger & V_2^\dagger & H_3 \end{pmatrix}, \tag{2}$$

where H_1 is the Coulomb Hamiltonian of the d-t system, H_2 is the free Hamiltonian of the n-α system,

$$H_3 = E_b|b><b| \tag{3}$$

is the Hamiltonian of the bare resonance, and V_1 and V_2 are the interactions of the two-particle channels d-t and n-α with the confined state ^{5}He*. Since the energy of the system, E, is reckoned from the d-t threshold, the n-α − d-t threshold difference $Q = 17.6$ MeV is included in H_2; E_b is the position of the bare resonance with the channel coupling switched off.

The scattering amplitude can easily be found by solving the Lippmann-Schwinger equation (see Ref. [10]), giving for the S-matrix element corresponding to d-t scattering

$$S_{11}(E) = e^{2i\delta_0(E)}\left(1 - \frac{i\Gamma_1(E)}{E - E_b - \mathcal{M}_1(E) - \mathcal{M}_2(E)}\right). \tag{4}$$

Here $\delta_0(E)$ is the Coulomb S-wave scattering phase shift, mass operators $\mathcal{M}_1$ and $\mathcal{M}_2$ are defined by

$$\mathcal{M}_a(E) = < b|V_a^\dagger(E - H_a)^{-1}V_a|b > \quad (a = 1, 2), \tag{5}$$

and

$$\Gamma_1(E) = 4m_1k_1|< dt, k_1|V_1|b >|^2 \tag{6}$$

is the width for the decay ^{5}He* $\rightarrow d + t$. The reduced mass and the relative momentum of the particles in channel 1 are $m_1 = m_d m_t/(m_d + m_t)$ and $k_1 = (2m_1E)^{1/2}$, respectively, and $|dt, k_1>$ is the S-wave solution of the scattering problem for the Hamiltonian H_1, normalized by the condition

$$< dt, k|dt, k' >= \frac{\delta(k - k')}{kk'}. \tag{7}$$

Similar definitions hold for the width $\Gamma_2(E)$ that corresponds to the decay ^{5}He* $\rightarrow n + \alpha$. Using the spectral representation for the Green's operator $(E - H_a)^{-1}$, one can express the mass operators as

$$\mathcal{M}_a(E) = \frac{1}{2\pi}\int_{E_a^{\rm th}}^{\infty}\frac{\Gamma_a(E')}{E - E'}dE', \tag{8}$$

where the integration is performed over the contour going along the real E axis from the channel threshold ($E_1^{\rm th} = 0, E_2^{\rm th} = -Q$) to infinity. For any reasonable choice of interaction V_a, the mass operator $\mathcal{M}_a(E)$ is an analytical function of the complex variable E having no singularities except for the cut going along the real E axis $(E_a^{\rm th}, \infty)$. The analytical continuation defines the multisheeted structure of the mass operators and, similarly, of the S matrix, as will be considered in more detail below.

We consider now the S matrix in the physical region of the energy variable E:

$$\begin{aligned} &S_{11}(E) = S_{11}(E + i\epsilon), \quad 0 \le E < \infty \ (d\text{-}t \text{ channel}), \\ &S_{12}(E) = S_{12}(E + i\epsilon), \\ &S_{22}(E) = S_{22}(E + i\epsilon), \quad -Q \le E < \infty \ (n\text{-}\alpha \text{ channel}). \end{aligned} \tag{9}$$

Using the spectral representation for the mass operator in Eq. (8), we can write it in the physical region in the form

$$\mathcal{M}_a(E + i\epsilon) = \Delta_a(E) - \frac{i}{2}\Gamma_a(E), \tag{10}$$

where the energy shift $\Delta_a(E)$ is defined by the principal-value integral

$$\Delta_a(E) = \frac{1}{2\pi}P\int_{E_a^{\rm th}}^{\infty}\frac{\Gamma_a(E')}{E - E'}dE'. \tag{11}$$

According to Eqs. (4), (6), and (8), the coupling of the

resonance with channels 1 and 2, which is primarily described by the operators V_1 and V_2, can be defined equivalently by means of the functions $\Gamma_1(E)$ and $\Gamma_2(E)$. We choose the width $\Gamma_1(E)$ to be of the form

$$\Gamma_1(E) = 4g_1^2 k_1 C_0^2(E)(1 + E/E_f)^{-2}, \tag{12}$$

where g_1 is the dimensionless constant of the ^{5}He* $-$ d-t coupling, $C_0^2(E)$ is the S-wave Gamow factor,

$$C_0^2(E) = \frac{2\pi\eta}{e^{2\pi\eta} - 1}, \quad \eta = \alpha m_1/k_1, \tag{13}$$

and the parameter E_f defines the range scale of the interaction V_1.

The energy dependence of the mass operator $\mathcal{M}_2$ describing the resonance coupling with the n-α channel can be neglected if we consider a narrow region in the vicinity of the d-t threshold ($E = 0-0.3$ MeV), since the distance Q between the thresholds is large in comparison with the characteristic scale determined by the range of the ^{5}He* $\rightarrow n+\alpha$ vertex. Therefore, given the energy dependence of the elastic width $\Gamma_1(E)$, the model involves three parameters: coupling strength g_1 for the ^{5}He* $-$ d-t vertex, the bare resonance position with the shift due to the ^{5}He*$-n$-α coupling taken into account, $E_0 = E_b - \mathrm{Re}\mathcal{M}_2$, and the inelastic width $\Gamma_2 = -2\,\mathrm{Im}\mathcal{M}_2$.

B. Determining the model parameters

The model parameters E_0, g_1, and Γ_2 have been determined from the best fit of the d-t scattering amplitude obtained from the R-matrix parameters given in Ref. [7]. The form-factor parameter E_f has been chosen to be $E_f = 2$ MeV, although reasonable fits can be obtained for any E_f within the interval 1.6–2.4 MeV. The best fit was obtained for the following values of the parameters:

$$\begin{aligned} &E_0 = 2.363 \text{ MeV}, \\ &\gamma = 2m_1 g_1^2 = 0.1602, \\ &\Gamma_2 = 0.3738 \text{ MeV}. \end{aligned} \tag{14}$$

Given the parameters E_0, g_1, and Γ_2, one can define two parameters E_1 and E_2, such that

$$E_1 - E_0 - \mathrm{Re}\mathcal{M}_1(E_1) = 0,$$

$$\Gamma_1(E_2) = \Gamma_2.$$

Their best-fit values are $E_1 = 79$ keV and $E_2 = 85$ keV. These parameters are helpful in the analysis of the S-matrix energy dependence. In particular, at $E = E_1$ the d-t nuclear scattering amplitude is purely imaginary, and if $E_1 \approx E_2$, the diagonal S-matrix element S_{11} is very close to zero at $E \approx E_1$ and the inelastic d-t cross section approaches the unitary limit. The parameters E_0, E_1, and E_2 can also be used, instead of E_0, g_1, and Γ_2, to specify the model considered. The results used from the R-matrix analysis allow one to define E_1 and E_2 with an accuracy better than 1 keV, while the parameter E_0 is correlated with the form-factor parameter E_f.

If we perform the fit using a more limited set of data (for example, only the d-t inelastic cross section) instead of the results of the R-matrix analysis that includes data from the three independent reactions, then two solutions are possible. The first (which is the "best") one is rather close to (14). The second set of parameters is

$$E_0 = 3.686 \text{ MeV}, \quad \gamma = 0.2513, \quad \Gamma_2 = 0.5479 \text{ MeV}, \tag{15}$$

which corresponds to $E_1 = 83$ keV and $E_2 = 82$ keV, so that $E_1 > E_2$, contrary to the case of Eq. (14).

Figure 1 shows the Argand diagram for the d-t nuclear scattering amplitude,

$$T(E) = \frac{S_{11}(E)e^{-2i\delta_0(E)} - 1}{2i}, \tag{16}$$

calculated from the parameters of Eq. (14) in comparison with the results of the R-matrix analysis [7]. The energy dependence of the astrophysical function $S(E)$ is shown in Fig. 2 compared with the experimental data [11–15], the calculated value of the spin-averaged reaction constant being $A_0 = S(0) = 11.8$ MeV b. Figure 3 shows the calculation and the experimental data [16] for the ratio

$$\xi = \left.\frac{d\sigma/d\Omega}{d\sigma/d\Omega_{\mathrm{Coul}}}\right|_{\theta=\pi/2} = \frac{1}{3} + \frac{2}{3}\left|\exp\left(-2i\eta \ln\sin\frac{\pi}{4}\right) - \frac{i}{2\eta}(1 - S_{11})\right|^2 \tag{17}$$

of the differential cross section for d-t scattering at $\theta_{\mathrm{c.m.}} = \pi/2$ to that of pure Coulomb scattering. The

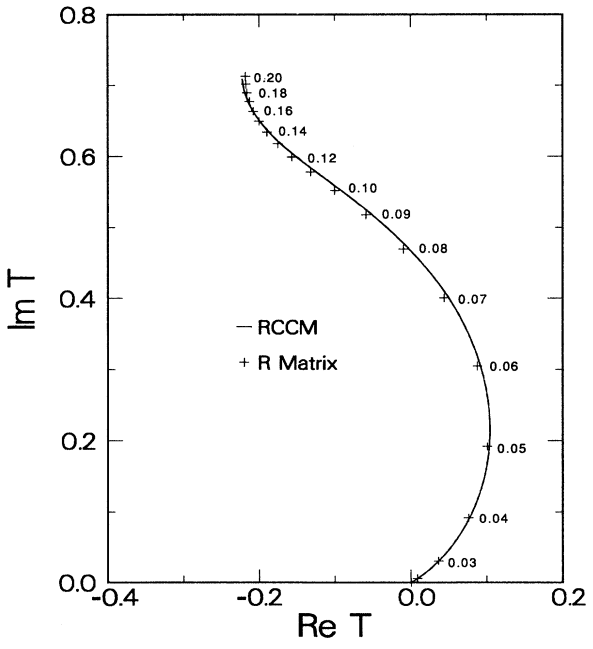

FIG. 1. The Argand diagram for the d-t scattering amplitude $J^\pi = \frac{3}{2}^+$ (solid line—RCCM, +—the R-matrix analysis [7]).

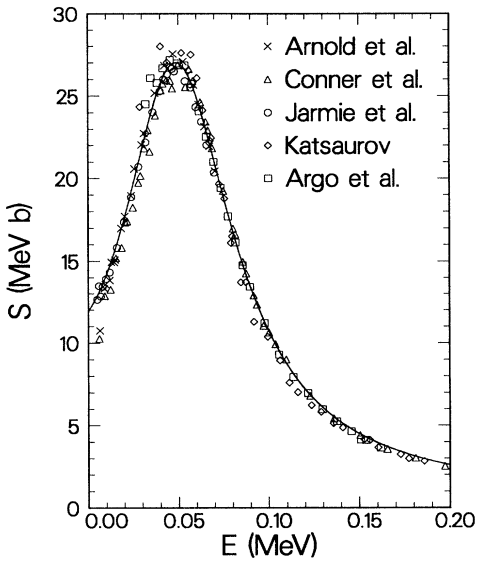

FIG. 2. The energy dependence of the astrophysical function $S(E)$ compared with the experimental data of Refs. [11] (×), [12] (△), [13] (○), [14] (◇), and [15] (□). For clarity, the data are shown without error bars.

very good agreement of the theoretical results with the experimental data and the R-matrix analysis shows that the coupled channel resonance model under consideration accounts for all the significant features of the $d+t \leftrightarrow n+\alpha$ interaction in the $^5\mathrm{He}(\frac{3}{2}^+)$ resonance region, and can therefore be used to investigate the nature of the resonance in more detail.

III. THE S-MATRIX POLES

In determining the analytical structure of the S matrix, we have two goals: First, given the physical parameters of the model, to find the poles that are responsible for the observable effects, and, second, to investigate the motion of these poles under variations of the coupling strengths. The latter allows us to make conclusions about the structure of the states associated with the physical poles even if the channel coupling is not weak.

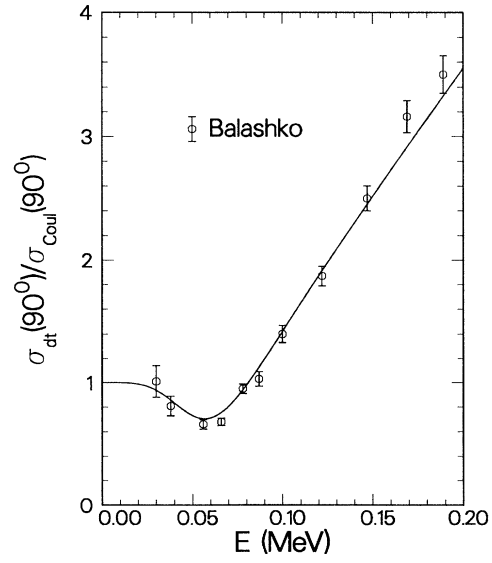

FIG. 3. The ratio of the differential elastic d-t cross section to that of pure Coulomb scattering in comparison with measurements by Balashko [16].

For a two-channel, two-particle system, the Riemann surface of the partial-wave S-matrix elements considered as a function of the energy variable E has four sheets, labeled in accordance with the signs of the imaginary parts of the channel momenta k_1 and k_2, as is shown in Table I. Besides the kinematical cuts due to the channel thresholds there may be dynamical cuts (the so-called potential or left-hand cuts) on the unphysical Riemann sheets U. For the resonance model under consideration, there is a potential cut due to the Coulomb interaction in the d-t channel which starts at the d-t threshold, as will be discussed briefly in the next section. There might also be dynamical cuts produced by the $^5\mathrm{He}^* - d$-t and $^5\mathrm{He}^* - n$-α coupling; however, with our choice of form factors [see Eq. (12)], there are no other singularities of dynamical origin besides the pole at $k_1 = -i\beta$, $\beta = (2m_1E_f)^{\frac{1}{2}}$. The far-away dynamical singularities related to the n-α channel play no role in the energy region considered and can be neglected. The effect of the confined channel, to which the compound (bare) state $^5\mathrm{He}^*$ belongs, is to create some additional poles on the unphysical sheets which, in the weak-coupling limit, appear in the vicinity of the initial pole position E_b as replicas of that on the physical sheet.

Given the mass operator determined by formula (8), the analytical continuation onto the unphysical sheets can be performed as follows: Let the energy point E move on the Riemann surface from the physical sheet P to the sheet U across the cut lying on the real E axis. When E is on the U sheet, one can continuously deform the contour to avoid its passing through the singularities at $E' = E$ and those of $\Gamma(E')$. If the function $\Gamma(E)$ is not singular at the point E, then the integral can be represented as the former integral along $(E_{\mathrm{th}}, \infty)$ *plus* the one along the circle centered at E, giving the following relationship between the mass operators on different sheets:

$$M^{II}(E) = M^{I}(E) - i\Gamma^{II}(E), \tag{18}$$

where superscripts I and II denote the physical and unphysical sheets for the two-particle channel considered. For example, calculating the S matrix on the sheet $U_{(1,2)}$, one has to use $\mathcal{M}_1^{II}(E)$ and $\mathcal{M}_2^{II}(E)$ in Eq. (4).

IV. RESULTS OF THE CALCULATION

A. Pole disposition

We have studied the analytical structure of the S matrix near the d-t threshold and found that the resonance

TABLE I. The labeling of the Riemann sheets.

Eden and Taylor [2]	P	$U_{(2)}$	$U_{(1,2)}$	$U_{(1)}$
Frazer and Hendry [4]	I	II	III	IV
Im k_1 (d-t)	+	−	−	+
Im k_2 (n-α)	+	+	−	−

pole is located at $E_R - i\Gamma_R/2 = (47 - i37)$ keV on the sheet $U_{(1,2)}$ and the shadow pole at $E_S - i\Gamma_S/2 = (82 - i3.4)$ keV on the sheet $U_{(2)}$ (see Figs. 4 and 5), both positions being in good agreement with the result of the R-matrix analysis [7]. The symmetry properties of the S matrix imply that the resonance and shadow poles have their counterparts located symmetrically with respect to the real E axis: One is at $E_R + i\Gamma_R/2$ on the sheet $U_{(1,2)}$ and the other at $E_S + i\Gamma_S/2$ on the sheet $U_{(2)}$. These two can be considered as far-away singularities since a path connecting any of them with some point in the physical region near the d-t threshold goes around the distant n-α threshold.

If we look for the poles using the set of parameters (15) corresponding to the limited data fit, then the resonance pole is found at almost the same position $E_R - i\Gamma_R/2 = (47 - i38)$ keV on the sheet $U_{(1,2)}$, but the shadow pole appears on the sheet $U_{(1)}$ at $E_S - i\Gamma_S/2 = (82 - i0.3)$ keV, rather than on the sheet $U_{(2)}$. The position of the shadow pole on the sheet $U_{(1)}$ (Γ_S value) is clearly sensitive to the particular selection of the data on the inelastic cross section involved in the fit. Thus, the contradiction between the results of Refs. [7] and [9] concerning the location of the shadow pole can be due to the fact that different sets of data have been used to determine the model parameters.

Besides the pairs of resonance and shadow poles, there is also the set of poles produced by the Coulomb interaction between d and t (antibound states) near the d-t threshold (see Fig. 4). A detailed discussion of these singularities will be given elsewhere (see also Ref. [9]).

B. Pole trajectories

In order to investigate the origin of the resonance $^5\mathrm{He}(\frac{3}{2}^+)$ we have traced the motion of the S-matrix poles as the parameters γ and Γ_2, which describe the coupling of the d-t and n-α channels with the bare $^5\mathrm{He}^*$ state, are varied. The trajectories of the resonance and shadow poles are shown in Figs. 4 and 5. As Γ_2 decreases from its physical value to zero, the resonance pole moves towards the physical region remaining on the sheet $U_{(1,2)}$ while the shadow pole crosses the real E axis moving from the sheet $U_{(2)}$ onto the sheet $U_{(1)}$. At $\Gamma_2 = 0$, the resonance and shadow poles lie symmetrically with respect to the real E axis at $E_R^0 \pm i\Gamma_R^0/2 = (61 \pm i19)$ keV. Because of unitarity constraints [2], any S-matrix pole located at some point E on the sheet $U_{(1)}$ or $U_{(2)}$ is accompanied by a zero of the diagonal matrix element S at the same value of E on the sheet $U_{(1,2)}$ or P, respectively. Therefore, the existence of a shadow pole close to the real E axis results in the striking observable effect of the inelastic cross section approaching its unitary limit $\sigma = \pi/k^2$, despite the fact that the shadow pole can be reached from the physical region only along a path going around the d-t threshold (see also Refs. [7] and [8]).

Although the inelastic cross section is large, the resonance coupling to the n-α channel can be characterized as weak because the resulting pole shift $(E_R - i\Gamma_R/2) - (E_R^0 - i\Gamma_R^0/2) = (-14 - i18)$ keV is small in comparison with the characteristic nuclear scale E_f and the distance between the thresholds Q. However, since

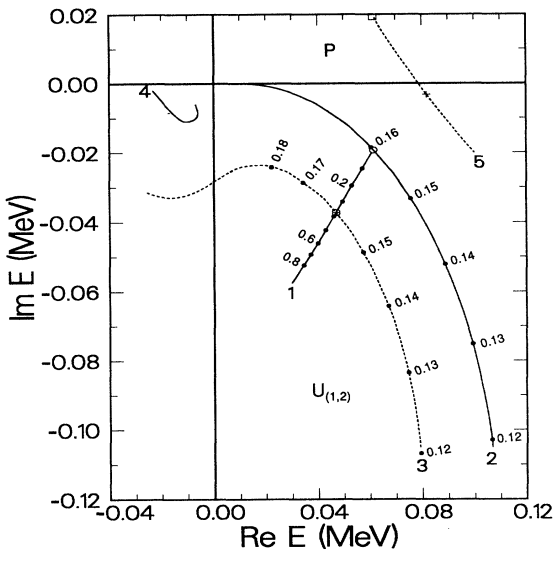

FIG. 4. The trajectories of the resonance pole on the sheet $U_{(1,2)}$: curve 1—the parameter Γ_2 is varied at the physical value of the $^5\mathrm{He}^*$ – d-t coupling strength γ [(⊕)—the pole location in the physical case, (⊙)—$\Gamma_2 = 0$]; curve 2—γ is varied at $\Gamma_2 = 0$; curve 3—the same as 2, but for the physical value of Γ_2; curve 4 shows the motion of the Coulomb pole corresponding to the antibound $1S$ state; curve 5—the motion of the zero of the diagonal matrix element S_{11} by varying Γ_2 at the physical value of γ [(+)—the physical case, (□)—$\Gamma_2 = 0$].

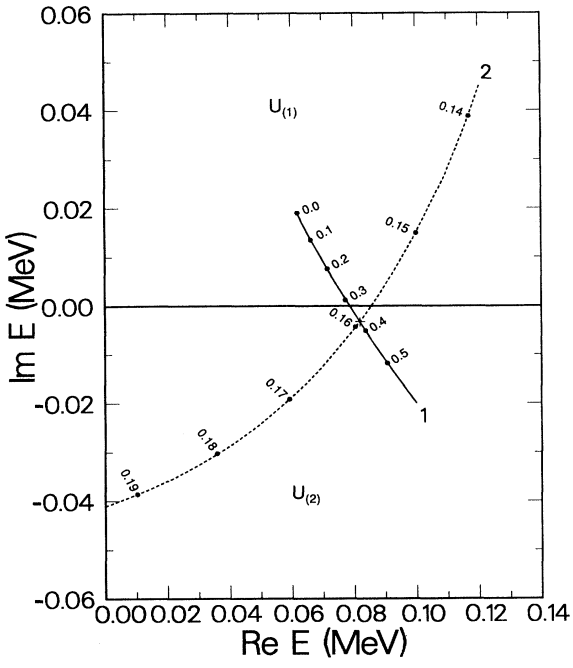

FIG. 5. The trajectories of the shadow pole on the sheets $U_{(1)}$ and $U_{(2)}$: curve 1—the parameter Γ_2 is varied at the physical value of the $^5\mathrm{He}^*$ – d-t coupling strength γ [(+) is the pole location in the physical case]; curve 2—γ is varied at the physical value of Γ_2.

the shadow pole is located very close to the d-t threshold, it can change sheets at rather small displacement $(E_S - i\Gamma_S/2) - (E_R^0 + i\Gamma_R^0/2) = (21 - i22)$ keV.

The motion of the poles with varying the ^{5}He* $-$ d-t coupling strength γ is shown in Figs. 4–6. As γ decreases from the physical value to zero, the pole associated with the resonance $^5\mathrm{He}(\frac{3}{2}^+)$ goes on the sheet $U_{(1,2)}$ along the trajectory ending at the point $E = -E_f$, which corresponds to the singularity of the form factor [see Eq. (6)]. The pole trajectory starting at $\gamma = 0$ from the position E_b of the bare ^{5}He* state moves from the physical region to the lower half-plane of the sheet $U_{(1,2)}$ (Fig. 6). Thus, the physical resonance $^5\mathrm{He}(\frac{3}{2}^+)$ appears as the coupled channel pole in the regime of the strong coupling between the d-t channel and the bare ^{5}He* state. [Coupled-channel (CC) poles [17] usually appear as a result of the strong coupling between two-particle (many-particle) channels. In our case their existence near the d-t threshold results from the strong coupling to the confined channel.] Because the pole originating from the bare state moves away from the resonance region, one can conclude that the physical resonance is the state associated predominantly with the d-t system. The quantitative description of the relative contribution of different configurations in the physical resonance can be obtained by using the probability sum rule.

V. THE PROBABILITY SUM RULE

In this section we present the derivation of the formula that allows one to calculate the probability of finding the confinement channel configuration within the resonance region. The starting point is the renormalized bare resonance propagator, which has the form

$$\mathcal{G}(E) = \frac{|b><b|}{E - E_b - \mathcal{M}_1(E) - \mathcal{M}_2(E)}. \tag{19}$$

Since there are no singularities except for possible bound states and the kinematical right-hand cuts on the physical sheet, Cauchy's integral formula gives

$$\int_C \mathrm{Tr}\mathcal{G}(E)dE = 0 \tag{20}$$

if the contour C is taken as shown in Fig. 7. Assuming that the mass operators vanish at infinity (which is valid for any reasonable choice of the widths), we get the probability sum rule

$$\frac{1}{2\pi}\int_{E_{\mathrm{th}}}^{\infty}[\mathrm{Tr}\mathcal{G}(E+i0) - \mathrm{Tr}\mathcal{G}(E-i0)]dE = 1 - \frac{1}{2\pi i}\sum_{\substack{\text{bound}\\ \text{states}}} \mathrm{Res}\ \mathrm{Tr}\mathcal{G}(E). \tag{21}$$

The integrand in the left-hand side of Eq. (21) gives the probability of finding the bare ^{5}He* state in the energy interval dE. Since there are no bound states in our model, the right-hand side of Eq. (21) is equal to 1. Formula (21) can also be interpreted as the projection of the closure relation onto the confined channel subspace. The energy region 0–0.2 MeV we have considered contributes only 12% of the normalization condition for the bare ^{5}He* state, confirming our conclusion about the predominant cluster nature of the resonance $^5\mathrm{He}(\frac{3}{2}^+)$.

VI. CONCLUSION

Within the framework of the RCCM we have investigated the pole structure of the $J^\pi = \frac{3}{2}^+$ resonance in

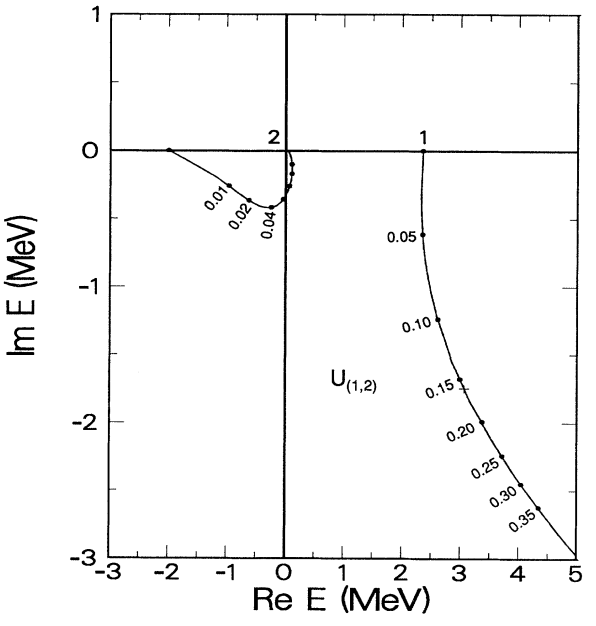

FIG. 6. The trajectories of the bare-state pole (1) and the resonance (CC) pole (2) on the sheet $U_{(1,2)}$, the ^{5}He* $-$ d-t coupling strength γ being varied at $\Gamma_2 = 0$.

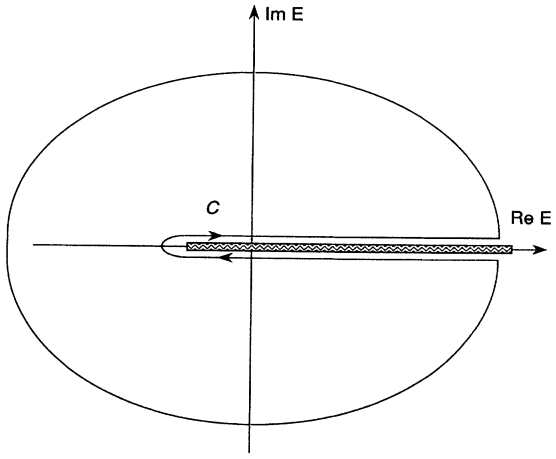

FIG. 7. Contour C for the integral in Eq. (20).

^{5}He, which dominates the ^{3}H$(d,n)^4$He reaction at low energies. The pole trajectories that result from varying the coupling strengths of the model potentials allow us to explore the dynamical origin of the resonance by extrapolating from the physical values back to the zero-coupling limit. In this way, the original structure of the resonance can be determined unambiguously within this model, since the physical disposition of the poles is indicative only in the weak-coupling regime.

We find that the physical ^{5}He$(\frac{3}{2}^+)$ resonance pole structure is well defined if one uses data from all three independent reactions near the d-t threshold, and is practically independent of the model used to obtain it. We have also seen that some ambiguities occur if a more limited data set is chosen, which could account for the differences in the location of the shadow pole found in Refs. [7] and [9]. From the pole trajectories and the probability sum rule, we have learned that the physical resonance is predominantly associated with the d-t channel. Further, we have found that the main and shadow poles responsible for the resonance arise from the singularity associated with the d-t channel coupling, rather than those associated with the bare ^{5}He* resonant state, or with the Coulomb singularities near the d-t threshold. At physical values, the n-α coupling is sufficiently strong to move the shadow pole from the sheet $U_{(1)}$, on which it originates, to the sheet $U_{(2)}$, but not strong enough to move it away from the d-t threshold.

The bare state ^{5}He* is essential in building up the physical resonance, but not in determining its properties as it approaches the region of the d-t threshold. This situation is typical for the strong-coupling regime in the case of spectrum rearrangement when the bare state (the "primitive") vanishes and leaves behind, like the grin of the Cheshire cat, the coupled channel state that determines the observable effects.

Our analysis also supports the approach to the investigation of the strong interaction effects in the $dt\mu$ mesic molecule developed in Ref. [18] within the framework of the (d-t, n-α) coupled channel model where the resonance ^{5}He$(\frac{3}{2}^+)$ was treated as being predominantly of d-t nature.

ACKNOWLEDGMENTS

Two of us (L.N.B. and V.E.M.) wish to thank Los Alamos National Laboratory for the hospitality they received during their stay at LANL. One of us (G.M.H.) is grateful for the hospitality of the Institute of Theoretical and Experimental Physics and the Kurchatov Atomic Energy Institute during his stay in Moscow. His part of this work was sponsored by the U. S. Department of Energy.

[1] F. Ajzenberg-Selove, Nucl. Phys. **A413**, 1 (1984).
[2] R. J. Eden and J. R. Taylor, Phys. Rev. **133**, B1575 (1964).
[3] M. Ross, Phys. Rev. Lett. **11**, 450 (1963).
[4] W. R. Frazer and A. W. Hendry, Phys. Rev. **134**, B1307 (1964).
[5] M. Kato, Ann. Phys. (N.Y.) **31**, 130 (1965).
[6] G. M. Hale, D. C. Dodder, and K. Witte (unpublished).
[7] G. M. Hale, R. E. Brown, and N. Jarmie, Phys. Rev. Lett. **59**, 763 (1987).
[8] B. C. Pearce and B. F. Gibson, Phys. Rev. C **40**, 902 (1989).
[9] B. M. Karnakov, V. D. Mur, S. G. Pozdnyakov, and V. S. Popov, Pis'ma Zh. Eksp. Teor. Fiz. **51**, 352 (1990) [JETP Lett. **51**, 399 (1990)].
[10] L. N. Bogdanova, V. E. Markushin, and V. S. Melezhik, Zh. Eksp. Teor. Fiz. **81**, 829 (1981) [Sov. Phys.—JETP **54**, 442 (1981)].
[11] W. R. Arnold, J. A. Phillips, G. A. Sawyer, E. J. Stoval, Jr., and J. L. Tuck, Phys. Rev. **93**, 483 (1954).
[12] J. P. Conner, T. W. Bonner, and J. R. Smith, Phys. Rev. **88**, 468 (1952).
[13] N. Jarmie, R. E. Brown, and R. A. Hardekopf, Phys. Rev. C **29**, 2031 (1984); R. E. Brown, N. Jarmie, and G. M. Hale, *ibid.* **35**, 1999 (1987).
[14] L. N. Katsaurov, Tr. Fiz. Inst. Akad. Nauk SSSR (in Russian) **14**, 224 (1962).
[15] H. V. Argo, R. F. Taschek, H. M. Agnew, A. Hemmendinger, and W. T. Leland, Phys. Rev. **87**, 612 (1952).
[16] Yu. G. Balashko, Tr. Fiz. Inst. Akad. Nauk SSSR (in Russian) **33**, 67 (1965).
[17] A. M. Badalyan, L. P. Kok, M. I. Polikarpov, and Yu. A. Simonov, Phys. Rep. **82**, 31 (1982).
[18] L. N. Bogdanova, V. E. Markushin, V. S. Melezhik, and L. I. Ponomarev, Yad. Fiz. **34**, 1191 (1981) [Sov. J. Nucl. Phys. **34**, 662 (1981)]; **50**, 1365 (1989) [**50**, 848 (1989)].